Journal of Solid State Chemistry 183 (2010) 895–900

Contents lists available at ScienceDirect

Journal of Solid State Chemistry

journal homepage: www.elsevier.com/locate/jssc

Structural phase transition and 5*f*-electrons localization of PuSe explored by *ab initio* calculations

Shouxin Cui [a,*], Wenxia Feng [a], Haiquan Hu [a], Zizheng Gong [b], Hong Liu [c]

[a] School of Physics Science and Information Technology, Liaocheng University, Liaocheng 252059, PR China
[b] Beijing Institute of Spacecraft Environment Engineering, Beijing 100094, PR China
[c] Institute of Earthquake Science China Earthquake Administration, Beijing 100036, PR China

ARTICLE INFO

Article history:
Received 11 December 2009
Received in revised form
6 February 2010
Accepted 14 February 2010
Available online 19 February 2010

Keywords:
Phase transitions
Electronic properties
Optical properties
FP-LAPW

ABSTRACT

An investigation into the structural phase transformation, electronic and optical properties of PuSe under high pressure was conducted by using the full potential linearized augmented plane wave plus local orbitals (FP-LAPW+lo) method, in the presence and in the absence of spin–orbit coupling (SOC). Our results demonstrate that there exists a structural phase transition from rocksalt (*B* 1) structure to CsCl-type (*B* 2) structure at the transition pressure of 36.3 GPa (without SOC) and 51.3 GPa (with SOC). The electronic density of states (DOS) for PuSe show that the *f*-electrons of Pu are more localized and concentrated in a narrow peak near the Fermi level, which is consistent with the experimental studies. The band structure shows that *B* 1-PuSe is metallic. A pseudogap appears around the Fermi level of the total density of states of *B* 1 phase PuSe, which may contribute to its stability. The calculated reflectivity $R(\omega)$ shows agreement with the available experimental results. Furthermore, the absorption spectrum, refractive index, extinction coefficient, energy-loss spectrum and dielectric function were calculated. The origin of the spectral peaks was interpreted based on the electronic structures.

1. Introduction

High pressure research on structural phase transformations of Pu monochalcogenides have been attracted interest, because these compounds display a variety of anomalous physical properties [1–3]. In contrast to the uranium and neptunium monochalcogenides, the Pu monochalcogenides (*B* 1 phase) do not show magnetic order and their lattice constants are anomalous small [4,5].

The phase stability of PuSe under high pressure has less been studied in experiments. X-ray diffraction studies demonstrated that there existed phase transition from *B* 1 structure to a rhombohedral structure up to 20 GPa, and finally it transforms to the *B* 2 phase around 35 GPa with a volume change of 11%. However, the details for this rhombohedral structure had not been reported [6]. By using an interionic potential theory with modified ionic charge, Srivastava et al. concluded that the transition pressure of $B1 \rightarrow B2$ for PuSe was 37.1 GPa with a 5.5% volume reduction [7]. To our knowledge, there are no density functional theory (DFT) studies of this phase transition pressure.

For the Pu monochalcogenides, the itineration or localization of 5*f* electrons has been a challenging problem for decades. The 5*f* electrons states are important for understanding the crystal structure and elastic properties. In addition, knowledge of the influence of 5*f* electrons on chemical bonding is crucial in understanding the physical properties of these materials. High symmetry for a crystal structure can be correlated with localized 5*f* electrons, and low symmetry goes along with itinerant 5*f* electrons [6]. The electronic structure of the Pu monochalcogenides has been studied both experimentally [2,8,9] and theoretically [10,11]. Electrical resistivity measurements for PuSe show a semiconductor-like crystal [2], which demonstrate that the Fermi energy (E_F) is situated in a small gap in the DOS. However, the measured magnetic susceptibilities dependence with the temperature indicated a relative large DOS at the E_F [8]. The theoretical calculations also gave contradictory results [6]. Considering localized 5*f* electrons, PuSe is an insulator and the absence of magnetic moment could be interpreted, but the corresponding f^6 configuration would result in a large lattice constant. However, assuming Pu trivalent, PuSe is metallic and the f^5 configuration would lead to be magnetic, which is contradict with experimental reports. The small lattice parameter had been obtained by assuming the itinerant 5*f* electrons. Moreover, the investigations of the other rare earth-contained Se crystals proved that these materials may be promising for the photoinduced nonlinear optics [12,13]. The investigations of the band energy structure of these materials may stimulate the corresponding investigations, particularly clarify role of *pf*

* Corresponding author. Fax: +86 635 8238055.
E-mail address: shouxincui@yahoo.com (S. Cui).

0022-4596/$ - see front matter Crown Copyright © 2010 Published by Elsevier Inc. All rights reserved.
doi:10.1016/j.jssc.2010.02.013

electron–phonon interactions near the phase transitions. With such a motivation, we aim to investigate the structural and electronic properties of PuSe compound by scalarrelativistic and full relativistic calculations. Such study is not only important to address the controversies in the electronic properties of PuSe compounds but also valuable for understanding the other Pu monochalcogenides.

2. Computational details

The calculations presented in this work are performed using the FP-LAPW+lo method as implemented in WIEN2K [14] code within the framework of DFT [15]. The exchange correlation potential within the GGA is calculated within the scheme of Perdew et al. [16]. In the FP-LAPW method, the wave function, charge density and potential are expanded by spherical harmonic functions inside non-overlapping spheres surrounding the atomic sites (muffin-tin spheres) and by a plane wave basis set in the remaining space of the unit cell (interstitial region). A mesh of $10 \times 10 \times 10$ and $11 \times 11 \times 11$ special k-points are taken in the whole Brillouine zone (BZ) for both B 1 and B 2 phases, respectively. The maximum l quantum number for the wave function expansion inside atomic spheres is confined to l_{max}=10. The convergence parameter $R_{MT}K_{max}$, which controls the size of the basis set in these calculations, is set to 9.5. The muffin-tin radius for Pu and Se were chosen 2.5 atomic units (a.u.). The cut-off energy, which defines the separation between the core and valence states, was set to -6.0 Ry. All these values have been chosen so as to ensure the total energy converged to better than 0.0001 Ry.

For the calculation of the optical properties (for the imaginary part of the dielectric tensor), a denser sampling of the BZ was needed, where we used $36 \times 36 \times 36$ k-point grid generated according to the Monkhorst-scheme [17]. The dielectric function $\varepsilon(\omega) = \varepsilon_1(\omega) + i\varepsilon_2(\omega)$ is known to describe the optical properties of the compounds, which is mainly connected with the electronic structures. The imaginary part $\varepsilon_2(\omega)$ of the $\varepsilon(\omega)$ is calculated from the momentum matrix elements between the occupied and unoccupied within selection rules. The real part $\varepsilon_1(\omega)$ of the $\varepsilon(\omega)$ can be derived from the $\varepsilon_2(\omega)$ using the Kramers–Kronig relation. And all other optical constants, such as the absorption spectrum, refractive index and reflectivity can be derived from $\varepsilon_1(\omega)$ and $\varepsilon_2(\omega)$.

3. Results and discussion

For calculating the ground states properties of PuSe, the total energies are calculated in scalarrelativistic (without SOC) [18] and in full relativistic (with SOC) [19] for both B 1 and B 2 phases with different volumes around the equilibrium cell volume V_0. The plots of calculated total energies versus reduced volume for PuSe in both phases are given in Fig. 1. It is worth mentioning from Fig. 1, that the B 1 structure is the most stable, which is consistent with experimental and theoretical works, and that the SOC reduces the total energy. However, it is not straightforward to get an accurate total energy when considering the SOC [20]. The calculated total energies are fitted to the Murnaghan's equation of state (EOS) [21] to determine the ground state properties such as equilibrium lattice constant a, the bulk modulus B and its pressure derivative B'. The calculated equilibrium parameters (a, B, B') for both structures are given in Table 1, together with available experimental [6,22,23] and theoretical results [4]. We have found that the equilibrium lattice parameters calculated in GGA+SOC

Table 1
Summary of calculated equilibrium lattice constants a, bulk modulus B (GPa) and its pressure derivative B' with and without SOC for B 1 and B 2 structures of PuSe, available experimental values and previous theoretical results are included for comparison.

	a (Å)	B (GPa)	B'
PuSe(B 1)			
GGA	5.642	89.01	4.321
GGA+SOC	5.756	77.192	5.278
Exp. [6]	5.7992	98	2.6
Exp. [22,23]	5.7934		
Ref. [4]	5.76	39	
PuSe(B 2)			
GGA	3.433	93.14	5.104
GGA+SOC	3.536	73.59	4.537

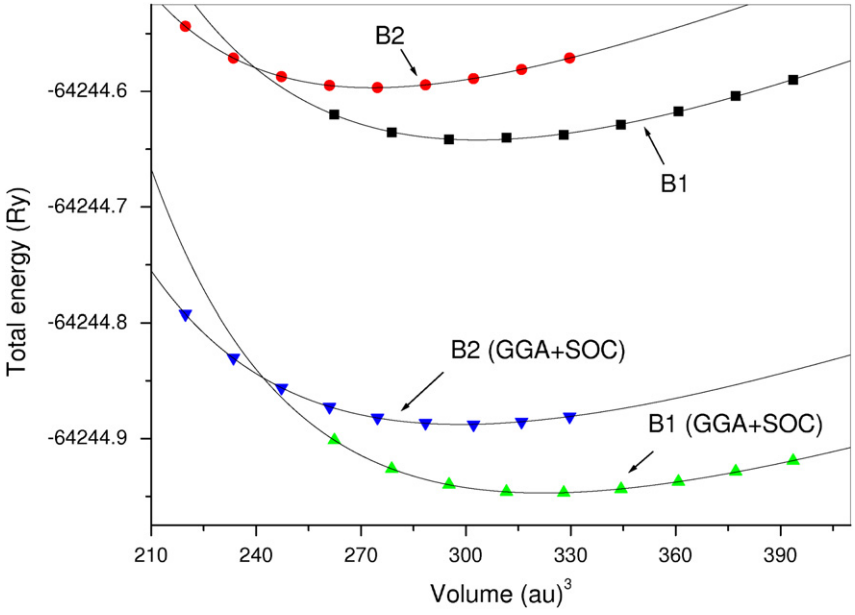

Fig. 1. Variation of total energy with unit cell volume in B 1 and B 2 structures for PuSe.

are in better agreement with the available experimental values compared to GGA. In addition, the calculated B without SOC is larger than calculated results with SOC.

Under compression, the calculation shows that PuSe will undergo a structural phase transition from B 1 to B 2 structure. One simple method for obtaining the zero-temperature transition pressure is from the slope of the common tangent of both E–V curves in Fig. 1. We can estimate the transition pressure (P_t) of 36.3 GPa (without SOC), which is in good agreement with the experimental value of 35 GPa [6], and other theoretical report of 37.1 GPa [7]. However, there are large discrepancy between the calculated P_t (51.3 GPa) with SOC and experimental results, and the SOC has a major effect on obtaining the P_t, it is most adequate not to include SOC in the total energy function for PuSe compound which have 6p states, which is consistent with the report of the limitation in implementation of the SOC for 6p electrons in full potential linear muffin-tin orbital (FP-LMTO) and FP-LAPW calculations [20].

The P–V relation calculated with the Murnaghan's EOS for PuSe solid is shown in Fig. 2. It can be seen that there is 6.3% volume reduction for the B 1-to-B 2 phase transition, and consistent with the theoretical report of 5.5% [7].

3.1. Electronic properties

In Fig. 3, we plot the electronic band structure both with and without SOC for B 1 phase of PuSe. The Fermi level (E_F) is set to

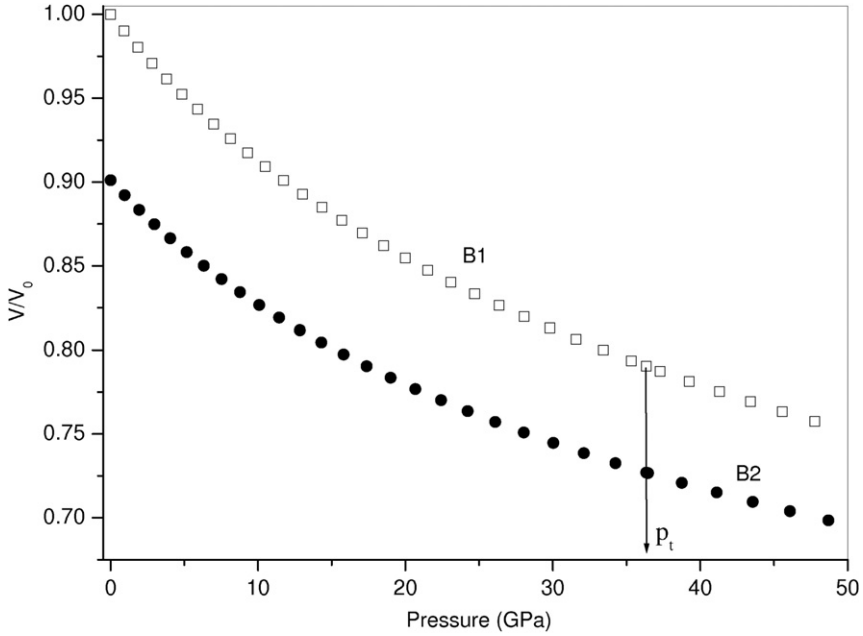

Fig. 2. Variation of relative volume V/V_0 for PuSe with pressure in B 1 and B 2 phases without SOC. V_0 is the zero pressure equilibrium volume of the B 1 phase, the arrows mark the calculated transition pressure P_t.

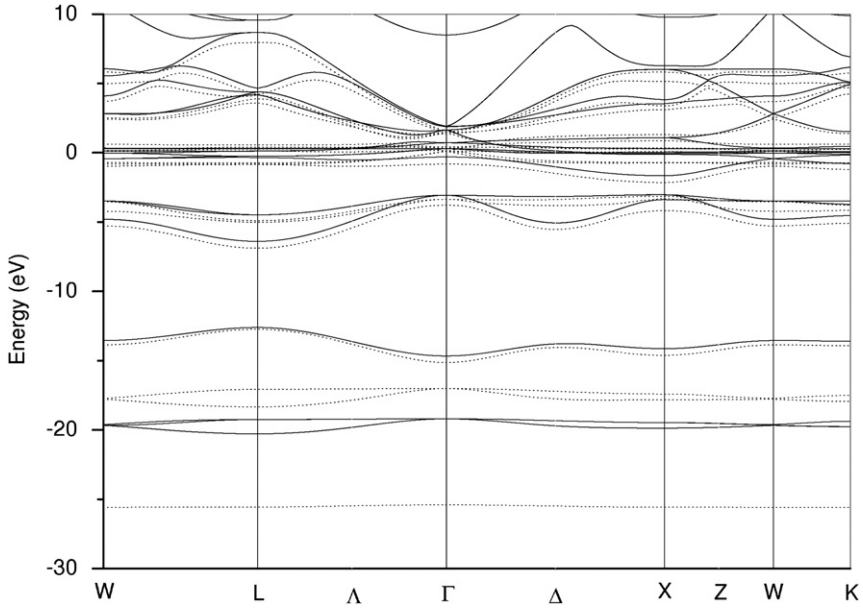

Fig. 3. Electronic band structure without (solid line) and with (dotted line) SOC for B 1-PuSe.

zero energy. It can be seen that there are some bands cross the E_F, which indicates the metallic behavior of *B* 1-PuSe. The total density of states (TDOS) and partial density of states (PDOS) calculated both without and with the SOC for the *B* 1 phase at 0 GPa are shown in Fig. 4(a) and (b), respectively. The metallic character of PuSe is confirmed by analysis of the TDOS. As seen in these figures, the major contributions to the occupied part of the DOS come from the Pu 6*p* and 5*f* and Se 4*s* and 4*p* states, which indicates that the 7*s* electrons of Pu transfer to the Se sites. In addition, from Fig. 4, we can see that almost all *f*- electrons (located in the energy from −1.0 to 1.0 eV) centered in the E_F, which indicates that the 5*f* states of Pu are more localized. This picture is in agreement with the X-ray photoelectron spectroscopy and high-resolution valence-band ultraviolet photoelectron spectroscopy spectra studies [9]. From Fig. 4(a) and (b), we can see that the SOC has a major effect on the semicore states of Pu 6*p* states, which spit up into $j=1/2$ and 3/2 subbands. The large split of these states is the root of the problem with the total energy functional, and the SOC pose a difficulty for the 6*p* electrons [20]. As a result of splitting, there are two different types of charge carriers and different effective masses.

The main differences between the DOS obtained in GGA and GGA+SOC approaches are the dramatic change at the E_F. In the absence of SOC (Fig. 4(a)), the DOS at E_f is very high. The effect of SOC is the strong decrease of the DOS at the E_F might be due to the spin orbit splitting of Pu 5*f* partial DOS into two disconnected

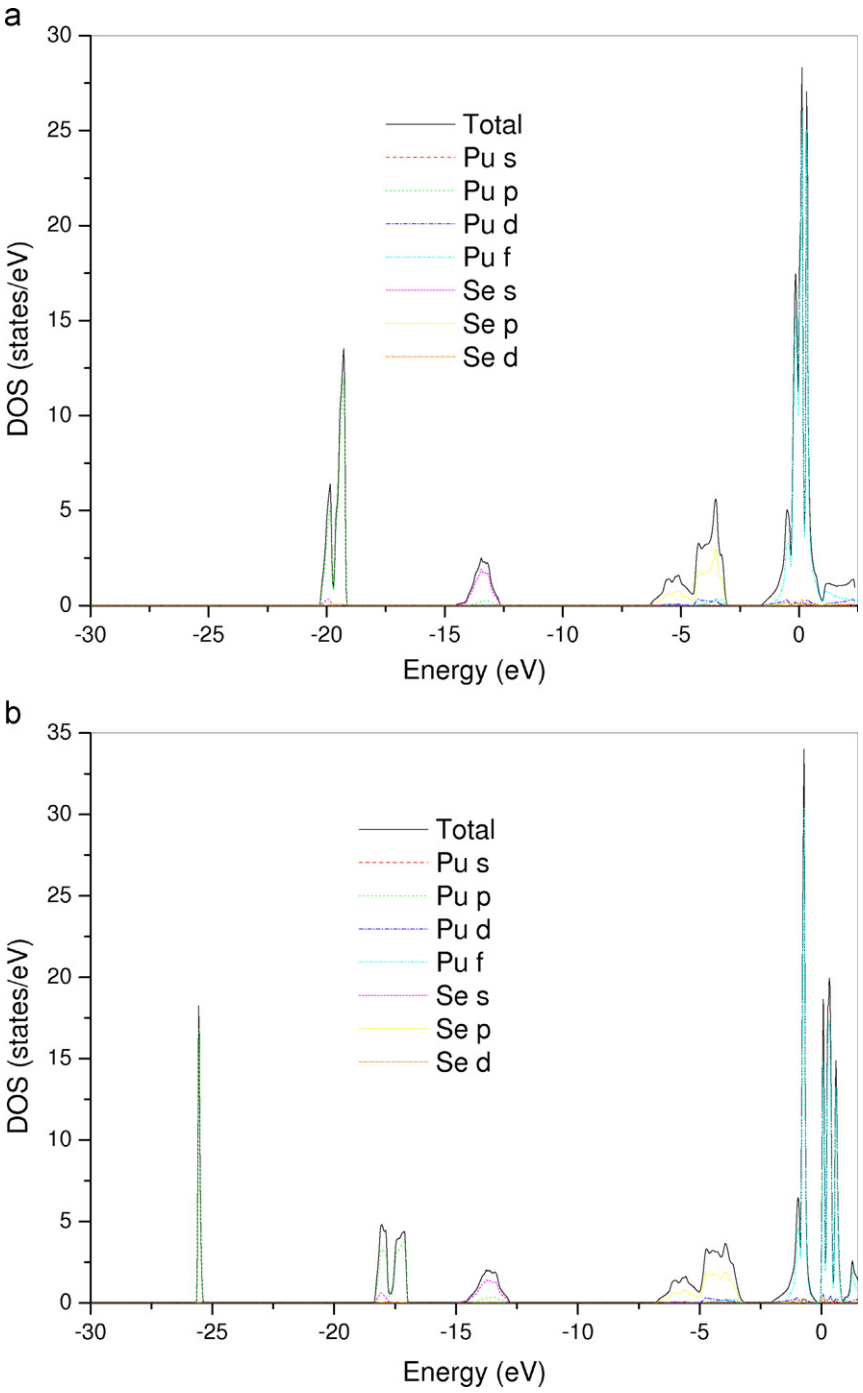

Fig. 4. Calculated TDOS and PDOS of PuSe for *B* 1 structure. (a) Without SOC, (b) with SOC.

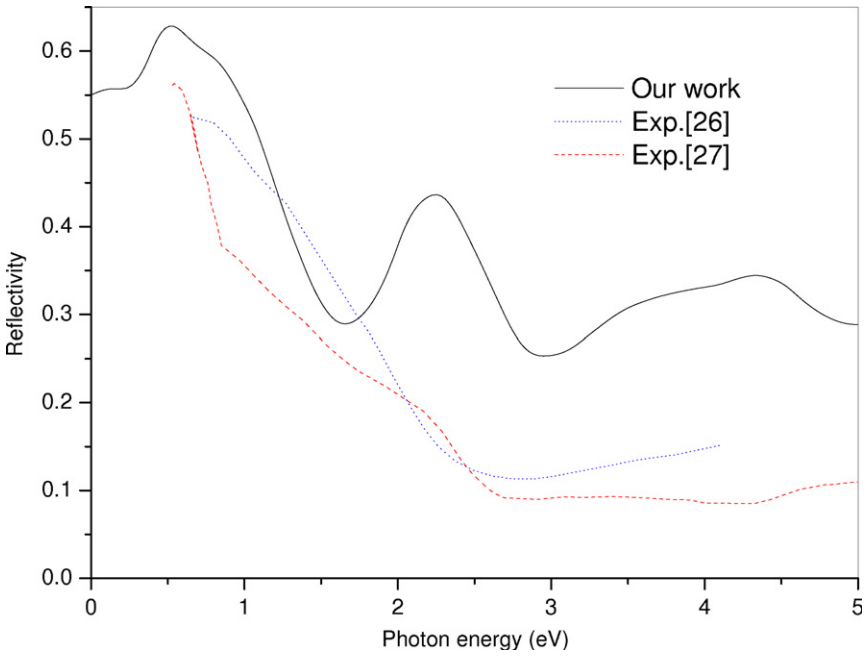

Fig. 5. Calculated reflectivity of PuSe for B 1 phase. The theoretical spectra are obtained for the ambient equilibrium lattice constant, a=5.756. The experimental data are from Ref. [26] (dotted line) and Ref. [27] (dashed line).

parts. These two peaks are corresponding to the j=5/2 and 7/2 5f subbands. The peak corresponding to j=5/2 is filled. Moreover, GGA+SOC DOS shows the existence of a pseudogap around the E_F, which is similar to what has been found for the PuTe system [5], where the pseudogap actually develops into a real gap giving semi-conducting behavior [4]. It has been indicated that materials with E_F located at a pseudogap in DOS will have a relative high stability (the situation with all bonding orbitals filled and all antibonding orbitals empty implies extra contribution to the stability) [24,25].

3.2. Optical properties

We considered the interband contribution in calculating the optical properties because of the metallic character for B 1 phase of PuSe. The calculated reflectivity can directly be obtained and compared to experiment. The reflectivity spectrum of PuSe was measured by Wachter [26] and Abraham et al. [27]. The experimental and calculated reflectivities for ambient equilibrium lattice constant at 0 GPa are shown in Fig. 5. We can see, from Fig. 5, there is a large peak at 2.25 eV, which is not observed in the experiment. Furthermore, there is a small peak at about 4.43 eV. In addition, our calculated reflectivity overestimated wholly the experimental reports.

The $\varepsilon_2(\omega)$ and $\varepsilon_1(\omega)$ as a function of the photon energy are plotted in Fig. 6. The imaginary part $\varepsilon_2(\omega)$ of the dielectric function is directly connected with the energy band structure. Peaks A (1.05 eV) and B (2.73 eV) correspond to the transition from Pu 5f of valence band (VB) to conduction band (CB). Peaks C (4.80 eV) and D (7.03 eV) correspond to the transition from Se 4p VB to Pu 5f VB and Pu 5f CB, respectively. Peaks E (9.37 eV) and F (9.92 eV) are ascribed to the transition of electron excitation from Se 4s VB to Se 4p VB. The calculated static dielectric constant $\varepsilon_1(0)$ was found to be 30.2.

The calculated results on the absorption spectrum, refractive index, extinction coefficient and energy-loss spectrum are shown in Fig. 7(a)–(d). The energy-loss spectrum describes the energy-loss of a fast electron traversing in the material, its main peak is generally defined as the bulk plasma frequency, which occurs

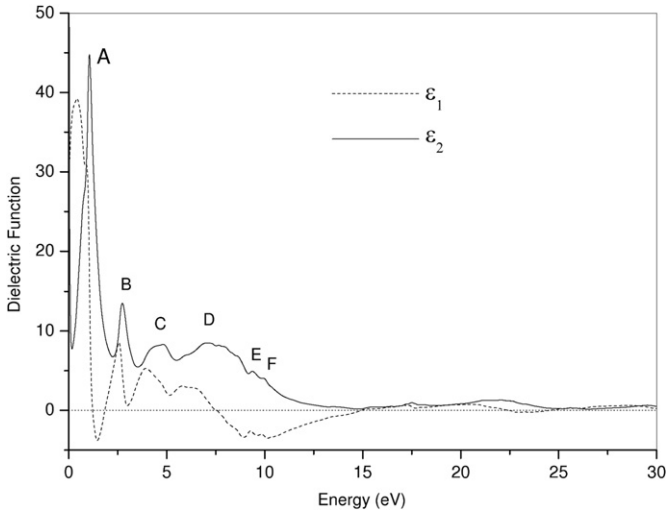

Fig. 6. Calculated imaginary part $\varepsilon_2(\omega)$ and real part $\varepsilon_1(\omega)$ of the dielectric function $\varepsilon(\omega)$ for B 1 phase of PuSe.

where $\varepsilon_2 < 1$ and ε_1 reaches the zero point, and the main peak at about 14.90 eV corresponds to a rapid reduction of the reflectance. In addition, the calculated static refractive index for photon energy 1.80 eV ($\lambda \approx 690$ nm) under 0 GPa is about 2.14.

4. Conclusions

We have studied the structural stability, electronic and optical properties of PuSe using the FP-LAPW+lo method both with and without SOC. In the absence of SOC, the $B1 \rightarrow B2$ phase transition occurs at the transition pressure of 36.3 GPa, with a volume discontinuity of about 5.5%, which is consistent well with the experimental reports. However, the inclusion of SOC overestimates the transition pressure by about 16.3 GPa. So, it is most adequate not to include SOC in the total energy function. However, adding SOC is probably preferable for the electronic

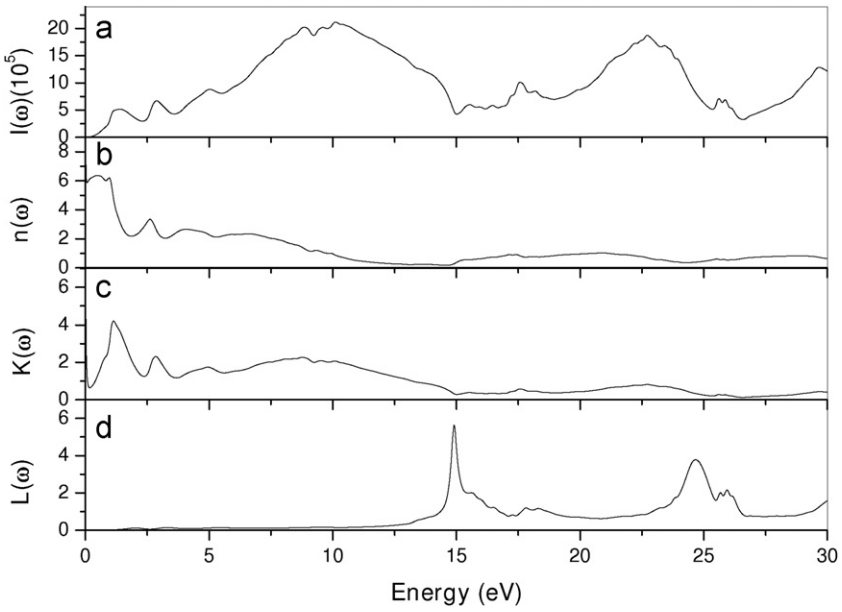

Fig. 7. Calculated optical constants for *B* 1-PuSe. (a) Absorption spectrum, (b) refractive index, (c) extinction coefficient and (d) energy-loss spectrum.

and optical properties, especially for these heavier compounds. Our calculated results demonstrate that there are limitations in implementation of the SOC for 6*p* states in FP-LAPW calculations.

Calculations of the DOS and band structure of PuSe show that *f*-electron is more localized and concentrated in a narrow peak near the Fermi level. The appearance of the pseudogap around the Fermi level of the total DOS may stabilize the *B* 1 phase of PuSe. Finally, the relations of the optical properties to the interband transitions were also discussed. For optical properties, there are only experimental reports of reflectivity for *B* 1 phase of PuSe. Therefore, we hope that our calculated results could serve as a reference for future experimental studies.

Acknowledgments

This work was financially supported by Science Foundation for Youth of Liaocheng University (no. X0810019). Special thanks should go to the Research Foundation of Shandong Provincial education department of China (no. J08LI13) and the Science Foundation for Distinguished Young scientist of Shandong Province (no. 2008BS04036). Finally, we also wish to thank referees for useful suggestions and comments.

References

[1] P. Wachter, F. Marabelli, B. Bucher, Phys. Rev. B 43 (1991) 11136.
[2] J.M. Fournier, E. Pleska, J. Chiapusio, J. Rossat-Mignod, J. Rebizant, J.C. Spirlet, O. Vogt, Physica B 163 (1990) 493.
[3] M. Mendik, P. Wachter, J.C. Spirlet, J. Rebizant, Physica B 186–188 (1993) 678.
[4] M.S.S. Brooks, J. Magn. Magn. Mater. 63–64 (1987) 649.
[5] P.M. Oppeneer, T. Kraft, M.S.S. Brooks, Phys. Rev. B 61 (2000) 12825.
[6] M. Gensini, E. Gering, S. Heathman, U. Benedict, J.C. Spirlet, High Press. Res. 2 (1990) 347.
[7] V. Srivastava, S.P. Sanyal, J. Alloys Compd. 366 (2004) 15.
[8] M. Mattenberger, O. Vogt, Phys. Scr. T 45 (1992) 103.
[9] T. Gouder, F. Wastin, J. Rebizant, L. Havela, Phys. Rev. Lett. 84 (2000) 3378.
[10] L. Petit, A. Svane, W.M. Temmerman, Z. Szotek, Eur. Phys. J. B 25 (2002) 139.
[11] M.S.S. Brooks, Phys. Scr. 35 (1987) 742.
[12] K. Nouneh, I.V. Kityk, R. Viennois, S. Benet, S. Charar, S. Paschen, K. Ozga, Phys. Rev. B 73 (2006) 035329.
[13] K. Nouneh, I.V. Kityk, R. Viennois, S. Benet, S. Charar, K.J. Plucinski, Mater. Res. Bull. 42 (2007) 236.
[14] P. Blaha, K. Schwarz, G.K.H. Madsen, D. Kvasnicka, J. Luitz, WIEN2K, An augmented plane wave + local orbitals program for calculating crystal properties, Karlheinz Schwarz, Techn. Universität Wien, Austria, 2001, ISBN 3-9501031-1-2.
[15] P. Hohenberg, W. Kohn, Phys. Rev. 136 (1964) B864.
[16] J.P. Perdew, K. Burke, M. Ernzerhof, Phys. Rev. Lett. 77 (1996) 3865.
[17] H.J. Monkhorst, J.D. Pack, Phys. Rev. B 13 (1976) 5188.
[18] D.D. Koelling, B.N. Harmon, J. Phys. C Solid State Phys. 10 (1977) 3107.
[19] A.H. MacDonald, W.E. Picket, D.D. Koelling, J. Phys. C Solid State Phys. 13 (1980) 2675.
[20] L. Nordström, J.M. Wills, P.H. Andersson, P. Söderlind, O. Eriksson, Phys. Rev. B 63 (2000) 035103.
[21] F.D. Murnaghan, Proc. Natl. Acad. Sci. USA 30 (1944) 244.
[22] O.L. Kruger, J.B. Moser, J. Phys. Chem. Solids 28 (1967) 2321.
[23] A.W. Mitchell, D.J. Lam, J. Nucl. Mater. 39 (1971) 219.
[24] P. Vajeeston, P. Ravindran, C. Ravi, R. Asokamani, Phys. Rev. B 63 (2001) 045115.
[25] Y.X. Wang, M. Arai, T. Sasaki, Appl. Phys. Lett. 90 (2007) 061922.
[26] P. Wachter, Solid State Commun. 127 (2003) 599.
[27] C. Abraham, U. Benedict, J.C. Spirlet, Physica B 222 (1996) 52.